Arctic Primary Aerosol Production Strongly Influenced by Riverine Organic Matter

Jiyeon Park,*,†,∇ Manuel Dall'Osto,‡,∇ Kihong Park,§ Jung-Hyun Kim,† Jongkwan Park,∥
Ki-Tae Park,† Chung Yeon Hwang,† Gwang Il Jang,† Yeontae Gim,† Sujin Kang,⊥ Sanghun Park,∥
Yong Keun Jin,† Seong Soo Yum,# Rafel Simó,‡ and Young Jun Yoon†

†Korea Polar Research Institute, 26 Songdomirae-ro, Yeonsu-gu, Incheon 21990, South Korea

‡Institut de Ciències del Mar, CSIC, Pg. Marítim de la Barceloneta 37-49, 08003, Barcelona, Catalonia, Spain

§Gwangju Institute of Science and Technology (GIST), 123 Cheomdangwagi-ro, Buk-gu, Gwangju 61005, South Korea

∥School of Urban and Environmental Engineering, Ulsan National Institute of Science and Technology, 50, UNIST-gil, Ulsan 44919,
South Korea

⊥Department of Marine Science and Convergent Technology, Hanyang University, 55, Hanyangdaehak-ro, Sangnok-gu, Ansan-si,
Gyeonggi-do 15588, South Korea

#Department of Atmospheric Sciences, Yonsei University, 50, Yonsei-ro, Seodaemun-gu, 03722, Seoul, South Korea

S *Supporting Information*

ABSTRACT: The sources of primary and secondary aerosols in the Arctic are still
poorly known. A number of surface seawater samples—with varying degrees of Arctic
riverine and sea ice influences—were used in a sea spray generation chamber to test
them for their potential to produce sea spray aerosols (SSA) and cloud condensation
nuclei (CCN). Our interdisciplinary data showed that both sea salt and organic matter
(OM) significantly influenced the SSA production. The number concentration of SSA
in the coastal samples was negatively correlated with salinity and positively correlated
with a number of OM tracers, including dissolved and chromophoric organic carbon
(DOC, CDOM), marine microgels and chlorophyll *a* (Chl-*a*) but not for viral and
bacterial abundances; indicating that OM of riverine origin enhances primary aerosol
production. When all samples were considered, transparent exopolymer particles
(TEP) were found to be the best indicator correlating positively with the ratio number
concentration of SSA/salinity. CCN efficiency was not observed to differ between the
SSA from the various samples, despite differences in organic characteristics. It is
suggested that the large amount of freshwater from river runoff have a substantial impact on primary aerosols production
mechanisms, possibly affecting the cloud radiative forcing.
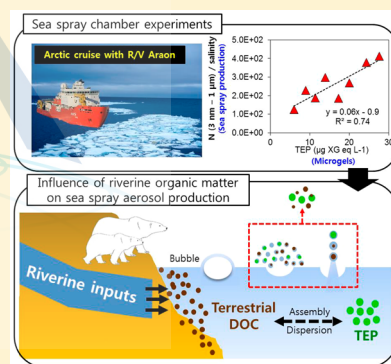
1.1. INTRODUCTION

The Arctic region is undergoing climate changes that are faster
than global average changes, a feature known as the Arctic
amplification.[1] Satellite passive-microwave data indicate that
Arctic sea ice extent has decreased at a rate of $51.5 \pm 4.1 \times 10^3$
$km^2\ yr^{-1}$ between 1979 and 2010.[2] Due to the diminishing sea
and the consequent increase in the ocean exposure to wind
friction, the Arctic Ocean can be one of the important
contributors to the ambient atmospheric aerosols. Marine
aerosols are either emitted directly from ocean surface via
bubble bursting (i.e., primary marine aerosols or sea spray
aerosols (SSA)) or formed by the oxidation of plankton-
emitted biogenic volatile organic compounds (i.e., secondary
marine aerosols).[3−5] Both aerosol types can significantly affect
the global radiation balance,[6] cloud formation (by acting as
cloud condensation nuclei (CCN) and ice nuclei (IN)),[7,8] and
the microbial cycle[9,10]

A number of field studies have provided evidence for the
presence of organics in the marine aerosol.[3,11−15] Sea salts
(produced by primary process) were proposed to be a major
component of SSA particles larger than 1 *μ*m, whereas the
organic fraction (produced by both primary and secondary
processes) increased up to ∼80% in the submicron aerosol
mass during a phytoplankton bloom.[11,12] A significant
percentage of the organic mass fraction was observed in the
central Arctic Ocean.[15−20] The identified organics were mainly
of primary biological origin such as primary saccharides (mean
46%), followed by secondary aerosol components (mean
21.6%).[18] In addition, the organic hydroxyl concentration was
correlated to submicron Na concentration, a sea salt tracer, and

wind speed in the Arctic atmosphere, indicating their direct association and probable primary formation.[17] However, since the Arctic is a complex mosaic of interconnected environments that includes sea ice, ocean, river, and land,[21−23] the sources of primary marine organic aerosols and their effects on Arctic climate are far from being resolved.

Seawater contains various organic matter (OM) pools and sources such as phytoplankton (typically quantified by the common tracer chlorophyll *a*), bacteria, viruses, dissolved organic carbon (DOC), transparent exopolymer particles (TEP), and coomassie stained particles (CSP).[9,24,25] The composition and behavior of SSA particles are greatly dependent on the chemical and biological composition of seawater.[24,25] To date, Chl *a* has been widely used as a proxy for phytoplankton biomass to explore influences of oceanic biological activity on SSA properties, because Chl *a* can be derived from satellite observations.[3,11,26] Positive correlations between satellite-derived Chl *a* and the organic fraction of SSA were observed in the northeast Atlantic.[11] Conversely, Quinn et al. (2014) reported that organic mass fractions of SSA particles were weakly correlated with satellite-derived Chl *a* levels in the northwest Atlantic and Pacific California. Instead, they suggested that DOC in seawater might be responsible for the OM enrichment in SSA.[27] Other studies have provided evidence for the transfer of bacteria and viruses from the sea surface into the atmosphere via bubble bursting.[28−30] This suggests that SSA and properties are influenced not only by phytoplankton productivity but also by other biological factors. Identifying these factors across environmental conditions is crucial to better calculate the organic enrichment of SSA, implement it in regional models, and reduce uncertainties in the impact of SSA on Arctic climate.

It has been suggested that ocean-derived OM enrichment in SSA particles plays an important role in determining CCN concentrations.[11,25,32−36] However, the actual impact of marine OM on CCN activity is largely uncertain due to the complex mixing state of SSA particles.[36] Ovadnevaite et al. (2011) found that OM-rich aerosols were associated with high CCN concentrations in marine air masses of the northeast Atlantic, and suggested that this might be due to the presence of marine hydrogels in seawater.[11,31] However, aerosol chamber experiments have reported that OM in SSA particles led to a small decrease in CCN concentration due to the hydrophobic properties of biogenic organics.[32−34] Field studies also showed no differences in the CCN activity of SSA particles, regardless of phytoplankton blooms over very different ocean regions.[27] Modeling studies have estimated that emissions of organic aerosols in SSA particles have led to a small global increase of 1.3% in CCN concentrations and a decrease of 0.09 W m^{-2} in aerosol indirect negative forcing.[35]

To investigate the connection between SSA properties and seawater OM in the Arctic, we conducted aerosol-generation chamber experiments onboard the Korean icebreaker R/V *Araon*. SSA particles were produced in a sea spray tank from three types of surface seawater samples, according to their distance from the shore and the depth of the water column: surface ocean (0−1 m) collected (a) in the Coastal Sea (CS), (b) in the Shallow Ocean (SO), and (c) in the Deep Ocean (DO). OM indicators measured were Chl-*a*, bacteria, viruses, DOC, chromophoric DOM (CDOM), fluorescent DOM (FDOM), dissolved organic nitrogen (DON), TEP, and CSP. Simultaneously, physical properties of SSA, including size distributions and CCN activity, were determined. This

study enabled us to establish the relationships between concentrations of different types of Arctic marine OM and the number concentration and CCN behavior of SSA.

2. EXPERIMENTAL SECTION

2.1. Seawater Sample Collection. Seawater sampling was conducted in the Beaufort Sea of the western Arctic Ocean onboard the Korean icebreaker R/V *Araon* from 30 August to 11 September 2017. Surface seawater samples were collected at 9 stations (Figure S1 of the Supporting Information, SI), using a Conductivity−Temperature−Depth (CTD) rosette sampler equipped with 24 Niskin bottles. All seawater samples were taken from sea surface at a depth of ∼1 m by Niskin bottles. The surface water salinity and bottom depth at each station were measured by the CTD (SBE 911plus CTD)/rosette system. To examine the effect of seawater organics on SSA properties, 3 surface water samples from the coastal sea (CS 1−CS 3) (i.e., sampling depth: 0−1 m, salinity: 19−25 ‰, bottom depth: 38−150 m), 4 surface water samples from the shallow ocean (SO 1−SO 4) (i.e., sampling depth: 0−1 m, salinity: ∼27 ‰, bottom depth: 420−750 m), and 2 surface water samples from the deep ocean (DO 1 and DO 2) (i.e., sampling depth: 0−1 m, salinity: ∼27 ‰, bottom depth: 1217−1750 m) were collected (Table S1). Distances from DO and SO sites to the coast (69.28°N, −138.35°W) were 142.50 and 198.41 km, respectively. In a nutshell, all the seawater samples used for this study were collected from the surface (0−1 m) of the ocean. The terminology herein used (CS, SO, DO) is only meant to separate three different categories of surface seawater, to see the effect of freshwater input in the Arctic primary aerosol production.

2.2. Sea Spray Tank Experiments. SSA particles were produced onboard using a laboratory-scale sea spray tank. The tank and how it works has been described previously in more detail.[37] In brief, a 5 L tank was filled with 3 L of each seawater sample. The seawater was pumped into the tank at a rate of 1.8 L min^{-1}, using an aquarium pump. The water entered through the nozzle from the top of the tank, which produced a vertical jet of water by hitting the surface. This plunging-water jet system can closely mimic the air entrainment caused by an oceanic breaking wave.[14,37,38] To avoid any contamination from indoor air, air was pumped through a HEPA capsule filter (Pore size: 99.97% retention of 0.3 μm dispersed oil particulate aerosol) (Pall laboratory) into the tank at a flow rate of 11 L min^{-1}. The flow rate remained constant during the operation of the tank. All the experimental conditions (water flow rate, plunging water depth, etc.) were performed according to Fuentes et al. (2010) settings,[38] to reproduce bubble size distribution similar to that observed in the ocean. Before turning on the water jet, we confirmed that the aerosol concentration, measured with a condensation particle counter (CPC) (TSI 3776) in the air space of the tank, was zero during the first 5 min of each experiment, ensuring that there was no leaking and no background particles (i.e., blank measurements).[12] Each primary aerosol chamber experiments lasted approximately 2 h. SSA particles generated by this tank were dried using a series of diffusion dryers, and the size distribution (3−10 μm) and CCN concentration of the dried SSA particles were measured using the aerosol instruments described in section 2 in the SI.[39]

2.3. Quantification of Organic Matter in Seawater. For DOC and Chl *a* analyses, 0.7−2 L of seawater were filtered through a precombusted 0.45 μm glass fiber filter (GF-5,
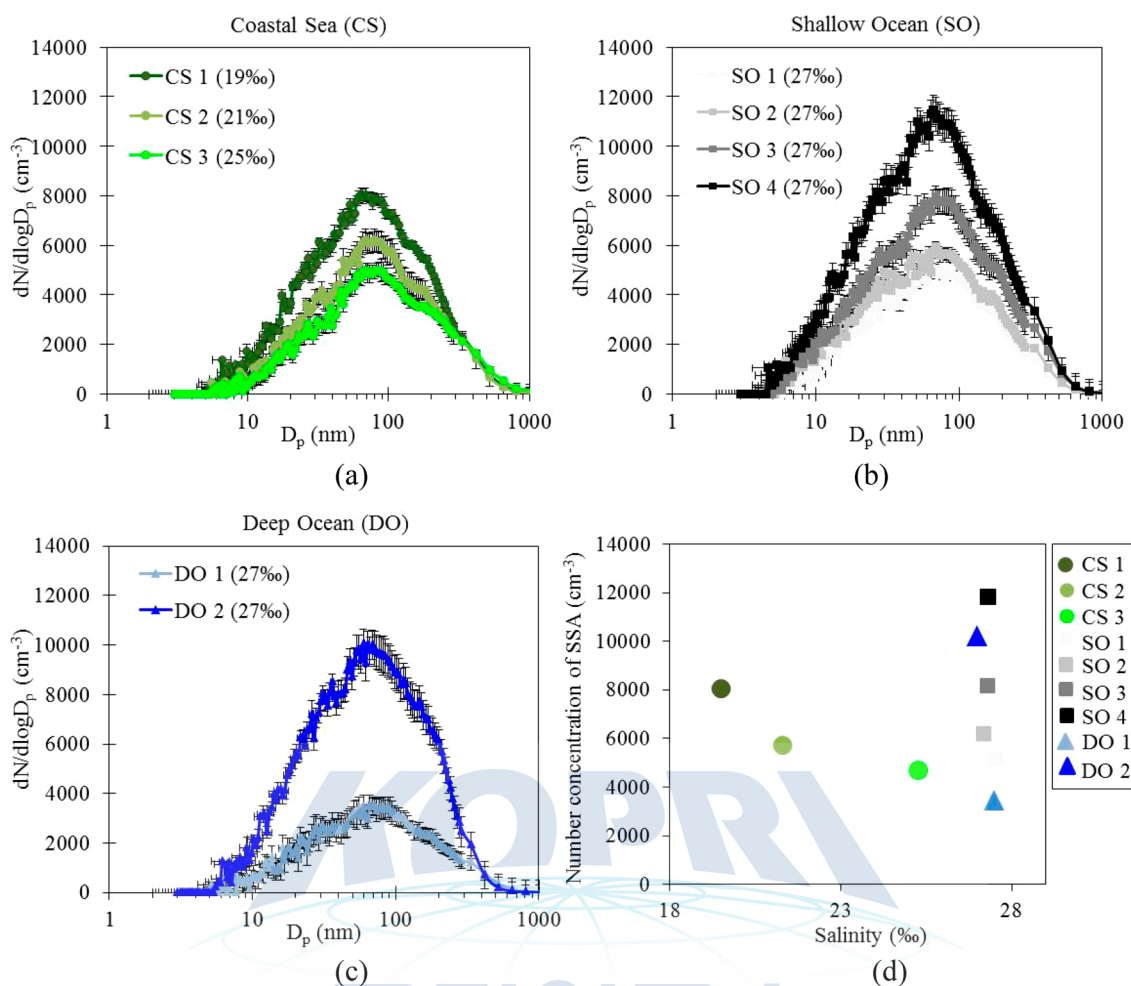
Figure 1. Number size distributions of SSA produced from surface seawater at (a) CS, (b) SO, and (c) DO, and (d) comparison between surface seawater salinity and total number concentrations of SSA particles for all samples (The circles, squares, and triangles s represent CS, SO, and DO samples, respectively).

Macherey Nagel, Germany). Filters were stored at −80 °C for pigment analysis after extraction. Filtrates were also sampled in 40 mL amber vials, with HgCl₂ for measurements of DOC concentration. Duplicates were taken for each sample. DOC concentration in the filtrate was measured on a Shimadzu TOC-V high-temperature combustion total organic carbon analyzer. All samples were systematically checked against deep seawater Consensus Reference Material (CRM) distributed by the Hansell Laboratory, University of Miami (supported by U.S. National Science Foundation). Pigments were extracted from the filter using 100% acetone in the dark at −20 °C for 24 h. Thirty μL of canthaxanthin was added as an internal standard. The extracts were transferred into 2 mL amber glass vials, after passing through 0.20 μm syringe filters (PTFE, AdvanTec, Japan). Chl *a* was analyzed using High Performance Liquid Chromatography (Agilent HPLC, 1200) with a Waters Symmetry C8 column, as described in Zapata et al. (2000).[40] Chl *a* was identified based on the retention time using spectral absorption at 350−750 nm, according to Jeffrey and Wright (1997).[41]

To determine the sources of DOC in seawater, chromophoric and fluorescent fractions of DOC (i.e., CDOM and FDOM, respectively) were further analyzed. Water samples (250 mL) were filtered using a 0.2 μm filter (AdvanTec, Japan) to remove particles larger than 0.2 μm. A UV/vis spectrometer

(Scinco, UV S-3100, Korea) with a 10 cm quartz cell was used to measure absorbance of the samples at 200−700 nm. Prefiltered Milli-Q water was used as the reference. The absorption wavelength at 375 nm was selected for an index of CDOM abundance. The absorption coefficients of CDOM at wavelength (λ) were calculated from the equation:

$$a_{CDOM} = \frac{2.303A(\lambda)}{l}$$

where A is the absorbance reading at wavelength λ, and l is the cell path length in meters.

FDOM was measured with a Varian Cary Eclipse fluorescence spectrometer. Three-dimensional excitation−emission matrices (EEMs) were constructed using the excitation spectra from 250 to 500 nm (10 nm intervals) and the emission spectra from 280 to 600 nm (10 nm intervals).[42] The EEM of deionized water was subtracted from analyzed samples to eliminate water Raman scatter peaks. The composition of the organic matter fraction was assigned into 4 groups (Figure S5); terrestrial humic substances peak (A) (EX: 260 nm, EM: 380−460 nm), the terrestrial fulvic substances peak (C) (EX: 350 nm, EM: 420−480 nm), the marine fulvic substances peak (M) (EX: 312 nm, EM: 380−420 nm), and the proteinaceous peak (T) (EX: 275 nm, EM: 340 nm).[43] The EEM images were acquired using the built-in function
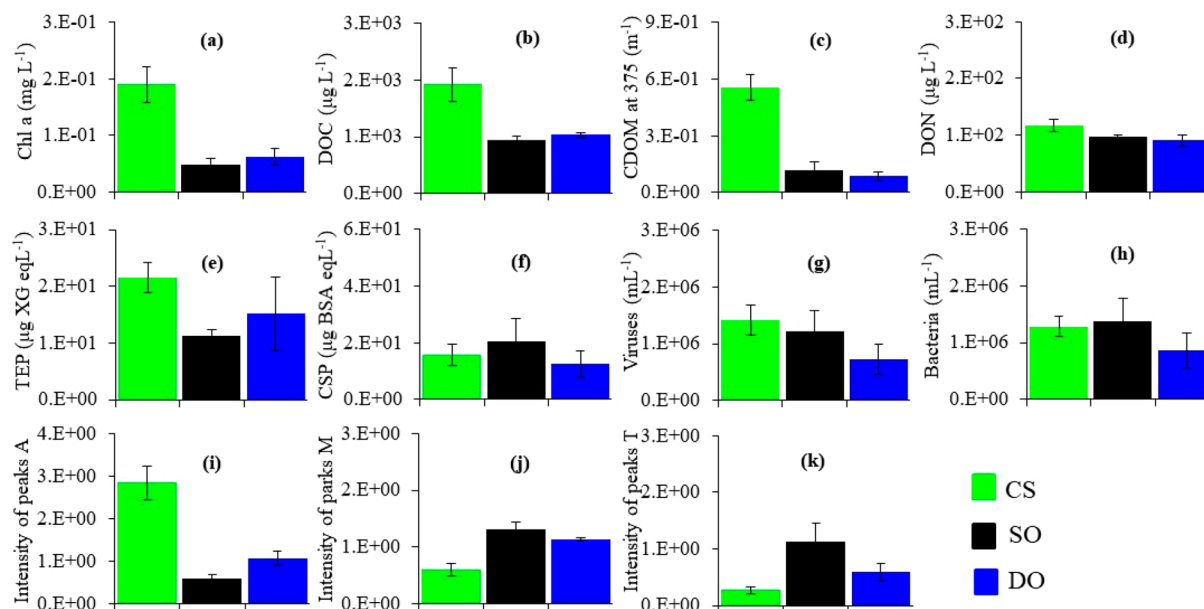
Figure 2. Average concentrations of (a) Chl *a*, (b) DOC, (c) CDOM, (d) DON, (e) TEP, (f) CSP, (g) viruses, (h) bacteria, and (i−k) relative fluorescence intensities in surface seawater sampled from CS, SO, and DO. (i), (j), and (k) represents relative fluorescence intensities of peaks A (terrestrial humic-like substance peak), peaks M (marine humic-like substance peak) and peaks T (proteinaceous peak), respectively.

"contourf" in MATLAB (R2018a, MathWorks, U.S.A.). Each contour interval represents 0.5 au

TEP and CSP were analyzed based on the colorimetric method.[44,45] Both TEP and CSP are defined as gel-like organic particles that are larger than 0.4 μm; that is, they are part of the particulate organic carbon (POC) pool. For the TEP measurements in surface seawater, duplicate samples (250 mL) were filtered using a polycarbonate membrane (25 mm diameter) with a pore size of 0.4 μm. The filters were stained with 500 μL of precalibrated (with xanthan gum s) Alcian Blue (AB) (0.02%, pH 2.5) for 5 s and rinsed with Milli-Q water. They were then soaked in 80% sulfuric acid for 3 h, and the absorbance of the extract was determined at 787 nm, using a Varian Cary spectrophotometer. To determine the CSP concentration in surface seawater, duplicate samples (250 mL) were filtered using Nuclepore membranes (25 mm diameter) with a pore size of 0.4 μm. The filters were stained with 1 mL of precalibrated (with a bovine serum albumin solution) Coomassie Brilliant Blue (CBB) (0.04%, pH 7.4) for 30 s and rinsed with Milli-Q water. They were extracted using the solution (3% sodium dodecyl sulfate (SDS) in 50% isopropyl alcohol) and were sonicated in a water bath (50−60 kHz) for 2 h at 37 °C. After the incubation, the absorption of the extraction solution was determined spectrophotometrically at 615 nm. For TEP and CSP analyses, duplicate samples were filtered and stained with AB and CBB on board the ship. Duplicate blanks (empty filters stained with AB or CBB) were also taken for each sample.

For measurements of viral and bacterial concentrations, seawater samples (10 mL) were fixed with 0.02 μm filtered formalin (final concentration of 2%) and were stored at −80 °C. Seawater samples (2.8 mL) were filtered through 0.02 μm pore size Anodisc filters (Whatman), and then the filters were placed on a 100-μL drop of SYBR Green I for 15 min in the dark.[46] Viral and bacterial abundances were counted at ×1000 magnification, using an epifluorescence microscope.

3. RESULTS AND DISCUSSION

3.1. Size Distribution of SSA Particles. Figure 1(a−c) shows the size distributions of SSA in the size range from 3 nm to 1 μm for the nine surface seawaters sampled from CS, SO, and DO. Sea surface salinity for CS, SO, and DO samples averaged 25.4 ± 3 ‰ (Table S1). Since the Mackenzie River is a major source of freshwater and provides nutrients and terrestrial components from the river into the Arctic Ocean,[47] CS samples represent low salinity condition (19−25 ‰). However, there was no difference in salinity between the SO and DO samples, with an average of 27.3 ± 0.2 ‰ (Table S1). The value appears to be lower compared with typical open ocean conditions (approximately 33.0 ‰), because the Arctic Ocean is strongly influenced by riverine inputs, sea ice, and melt waters.[48] The aerosol size distributions for CS, SO, and DO samples remained substantially stable during a given experiment, which lasted about 2 h. Number concentrations of SSA particles were significantly different among CS, SO, and DO samples (Figure 1), but the size distributions showed a similar shape (Figures 1 and S2), similar to previous studies published with the same system.[37] Aerosol size distributions data showed mainly four different size modes at approximately 26 nm (nucleation mode), 68 nm (Aitken mode), 188 nm (Accumulation mode), and 337 nm (Additional fourth mode).[44] A mode, at around 300 nm, was also observed by Selligri et al. (2006) and Fuentes et al. (2010) during bubble bursting chamber experiments. The 300 nm mode was interpreted as the result of a thicker bubble film where the bubbles are forced to break by the wind at the surface, when fail to burst upon reaching the air−water interface.[37] Number concentrations of SSA generated from costal samples (CS) changed considerably (4.68×10^3 to 8.03×10^3 cm^{-3}) with salinity, which ranged from 19 to 25 ‰ due to the influence of the freshwater outflow of the Mackenzie River (Figure 1 a). Conversely, SO samples had similar salinity (∼27 ‰) but led to different number concentrations of SSA (3.46×10^3 and 1.02×10^4 cm^{-3}) (Figure 1 b). DO samples also showed
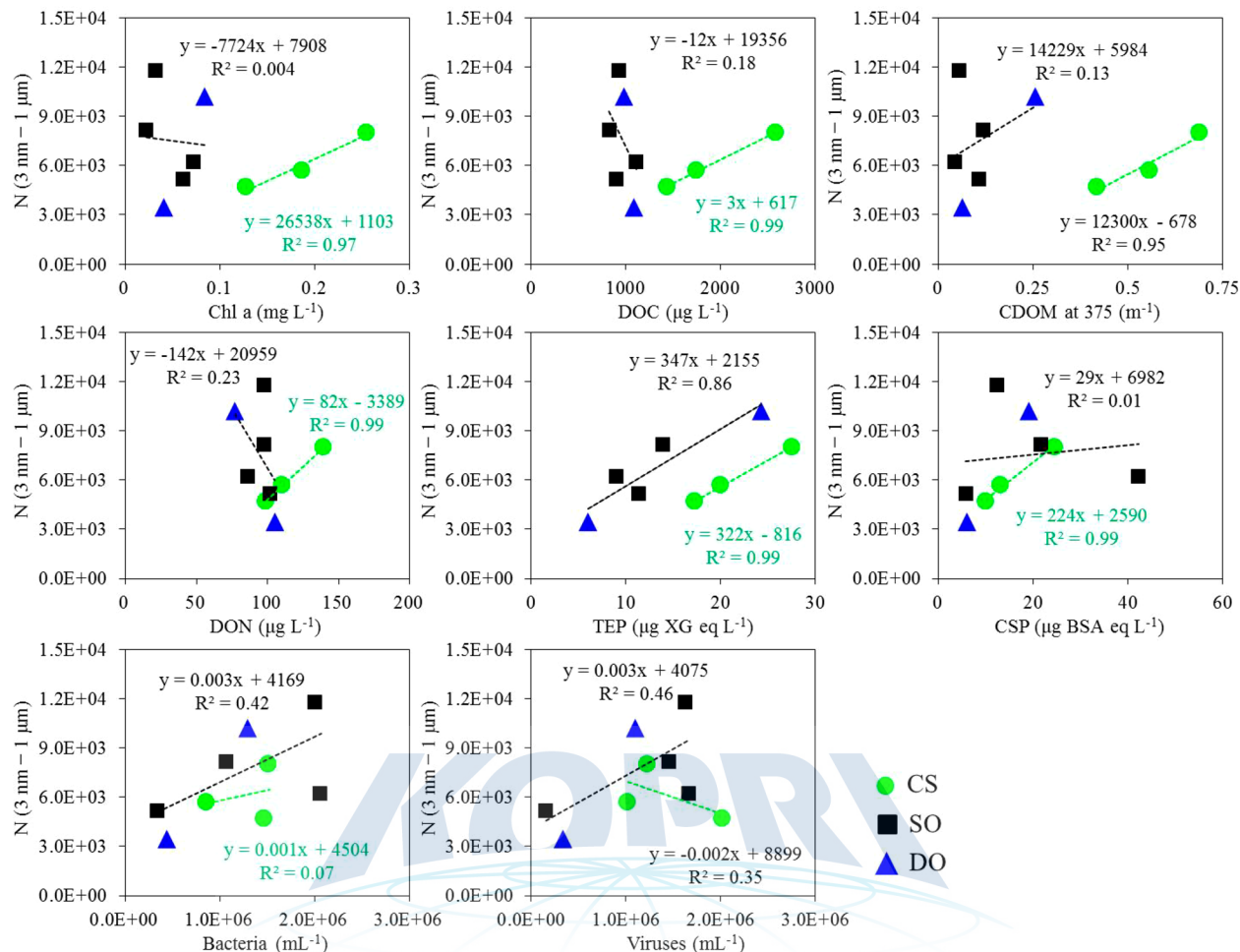
Figure 3. Relationships between total number concentrations of SSA particles (i.e., N (3 nm to 1 μm) and concentrations of various organic matter tracers in seawater samples from CS (green circles), SO (black squares), and DO (blue triangles). The regression for SO and DO samples was plotted altogether. All parts include 9 data points, but the part for the TEP vs SSA number have 8 data points due to a no evidence of duplication for TEP in the SO4 seawater samples.

drastic changes in number concentrations of SSA (5.17×10^3 to $1.18-10^4$ cm^{-3}) despite their similar salinity ($\sim$27 ‰) (Figure 1 c).

Figure 1 d shows the relationship between total number concentrations of SSA in the size range from 3 nm to 1 μm and surface seawater salinity for the entire set of samples. The inverse correlation between number concentration of SSA and salinity obtained for CS samples implies that less salinity results in the production of more SSA particles in the coastal region. Previous studies reported that salinity plays an important role in number concentrations of aerosols resulting from the bubble bursting processes under relatively low water temperature.[49−51] During the bubble bursting, higher salinity can produce higher numbers of bubbles including dissolved salt ions, leading to the higher number of SSA in air after crystallization with the drying process. Our striking results show the opposite pattern, therefore suggesting that seawater OM may have a much larger effect on the number concentration of SSA particles than that of salinity (see further discussion below).

3.2. Characterization of Organic Matter in Surface Seawater. Figure 2 shows average concentrations of OM tracers (Chl a, DOC, CDOM, DON, TEP, CSP, viruses, and bacteria) in the surface seawater samples from the CS, SO, and

DO sampling regions. All seawater samples were collected at a depth of $\sim$1 m (section 2.1). Chl-a and DOC concentrations in the coastal samples were 3.5 and 2.0 times greater than those in the offshore ocean samples, respectively. In particular, surface seawater sampled from station CS 1 (salinity: 19 ‰ and bottom depth: 38 m) contained the highest Chl a and DOC concentrations of all samples (0.25 μg L^{-1} for Chl a and 2583.0 μg L^{-1} for DOC) (Figure S3). The average values of DOC for CS, SO, and DO samples were 1919 $\pm$ 297 μg L^{-1}, 941 $\pm$ 61 μg L^{-1}, and 1033 $\pm$ 31 μg L^{-1}, respectively. Previous studies reported that DOC concentrations in the upper Arctic oceans (sampling depth: 1−80 m) varied from 800 μg L^{-1} to 1140 μg L^{-1}, regardless of time and space.[52−55] Our offshore DOC concentrations fall within this general range. The fraction of DOM that absorbs light at ultraviolet (UV) and visible wavelengths, referred to as CDOM,[23] has been used as a proxy for tracking portions of DOM, mainly for those derived from terrestrial inputs in coastal areas (i.e., a tracer of terrigenous DOM).[56,57] The highest CDOM concentrations (0.56 m^{-1}) were found in the CS samples (Figure 2c). DOC concentrations showed a strong positive correlation with CDOM concentrations ($R = 0.94$) (Figure S4a) and a negative correlation with salinity (Figure S4b), implying terrestrial inputs from the Mackenzie River in the coastal region

(especially for CS 1). The terrestrial DOC originated from rivers could be largely old and refractory.[58,59] Changes in DON concentration (e.g., a main source of reactive nitrogen in the surface ocean) in surface seawater samples from CS, SO, and DO were minor and insignificant.

TEP concentrations in the coastal samples were 1.6 times greater than those in the offshore ocean samples. Conversely, we found no significant differences in CSP concentrations. There was no clear trend either for viral and bacterial concentrations (Figure S3), which were within the range previously reported (10^5-10^6 mL^{-1}) in the southeastern Beaufort Sea (sampling depth: < 2 m) during the Canadian Arctic Shelf Exchange Study (CASES).[60] DOC polymers in seawater form nanogels due to their tangled topology, and then grow by annealing to form microgels.[45,61,62] The resulting microgels contain polysaccharides, proteins, and nucleic acids. TEP are carbon-rich particles (primarily polysaccharide), and CSP are protein-containing particles.[51] In general, TEP formation is enhanced at higher salinity, because microgels are stabilized by Ca^{2+} and Mg^{2+} ionic bonds.[56,63] Here, high TEP concentrations were found in the coastal sample with low salinity (Table S1). This could be due to TEP formation by aggregation of colloids carried by riverine discharges. This is supported by the higher concentrations of DOC and CDOM observed in the CS stations under the river influence.[55]

To further ascertain the composition and origins of DOC, excitation−emission matrix (EEM) fluorescence spectra of the Arctic surface water were measured (Figure S5). The relative fluorescence intensities of peaks A at ex/em = 260/450 nm (terrestrial humic-like), M at ex/em = 300/400 nm (marine humic-like), and T at ex/em = 270/340 nm (protein-like) obtained from the excitation/emission pairs are presented in Figure 2 (i-k). A strong peak A in the region of terrestrial humic-like fluorophores was observed in the CS samples (Figure 2 (i). In contrast, an obvious peak M, which is considered as marine humic-like fluorophores, was found in SO and DO samples, (Figure 2 j). This suggests that high DOC levels in coastal samples were related to a terrestrial source, whereas lower DOC levels in ocean samples were related to a marine source. A significant peak T of protein-like DOM - especially in the SO 2 sample (i.e., surface seawater sample from shallow ocean; salinity: 27 ‰)—was observed in the EEM spectra (Figures 2k and S5). The highest concentrations of CSP and bacteria were also found in the SO 2 sample (Figure S3). Thus, the similarity in variations among fluorescence peaks, CSP, and bacteria in the SO 2 sample suggests that bacterial production (through cell lysis or death) may be a source of protein-rich CSP in the ocean.

3.3. Effects of Surface Seawater OM on SSA Properties. Figure 3 shows the relationship between number concentration of SSA particles and OM tracers in seawater. In the coastal samples (salinity <25 ‰), number concentration of SSA particles was significantly and positively correlated with DOC, CDOM, DON, TEP, Chl a, and CSP abundances; however, there were no correlations with viral and bacterial abundances. This provides strong evidence that, although abundances of bacteria and viruses in seawater are high (10^5-10^6 mL^{-1}), SSA production is predominantly influenced by DOC, TEP, and Chl a in coastal waters, where riverine inputs are dominant. Furthermore, when all samples were considered, the ratio TEP/salinity was a good predictor of number concentration of SSA particles (Figure S6). Alpert et al.[14] also found that number concentrations of SSA

generated in laboratory mesocosm experiments with Atlantic seawater were—although weakly—positively correlated with TEP. Major sources of DOC in coastal seawater include microbial productivity (e.g., release of extracellular products by phytoplankton, bacterial and viral lysis, sloppy feeding of zooplankton, and cell senescence), and soil-derived humic materials transported by rivers.[57,64] The DOC (size range: < 0.4 μm) released by phytoplankton and discharged by riverine outflow abiotically assembles to form polymer gels, especially TEP (size range: > 0.4 μm), due to ionic bonds. Eventually, riverine OM can be emitted from the sea surface into the atmosphere via the bubble bursting of breaking waves. Therefore, the coastal region under the influence of riverine discharges may play an important role in the production of SSA in the Arctic. For instance, Miyazaki et al.[65] reported that humic-like DOC in surface seawater (sampling depth: ~2 m) would be more incorporated into SSA particles than protein-like DOC in subarctic coastal regions. Aller et al.[15] also demonstrated that both TEP and CSP in surface ocean water can be aerosolized with SSA particles under field conditions.

In the offshore ocean samples (salinity >25 ‰), there were no clear correlations between number concentration of SSA particles and certain types of OM tracers such as Chl-a, DOC, CDOM, DON, and CSP in the offshore ocean samples (Figure 3). This is due to the different physical and chemical properties of OM (e.g., abundance and diversity) from riverine inputs and from marine plankton. For example, differences of DOM and POM concentrations in the offshore ocean samples were insufficient to regulate the production of SSA particles compared to the coastal sample (section 3.2).[11,66] Conversely, number concentration of SSA particles correlated with TEP, bacteria, and viruses in the ocean sample, suggesting their potential contributions to primary aerosol production. Typically, higher salinity produced higher numbers of SSA particles, as previously demonstrated by Mårtensson et al. (2003)[49] and Park et al. (2014).[50] By contrast—in this study—at higher salinities (i.e., 27 ‰ in offshore ocean samples), the number concentration of SSA varied largely (Figure 1 d) with variations in the numbers of biological particles in the ocean (TEP, bacteria, and viruses). At lower salinities (i.e., coastal samples), the number concentration of SSA varied and even reached values equivalent to those at higher salinity (Figure 1d) because of the presence of riverine OM (DOC and TEP). In a nutshell, our Arctic primary aerosol chamber data shows that OM greatly affects the aerosol production mechanisms. Out of all the OM tracer herein used, we found that TEP was the best surrogate to correlate OM with aerosol particle fluxes, independently of the amount of sea salt contained among different surface water samples.

3.4. CCN Activities of SSA Particles. Figure 4 a compares the CCN concentrations of SSA particles generated from CS, SO, and DO samples at different supersaturation conditions. No statistically robust differences can be seen among the three different groups. Figure 4b illustrates the CCN activity of SSA particles generated from CS, SO, and DO. The CCN activation ratios also show no differences between coastal (CS) and open ocean (SO and DO) sea surface samples at the same supersaturation conditions. When the CCN concentrations of individual samples are correlated with different variables (Figure S7), similar trends reported in Figure 3 can be seen. Although seawater OM can noticeably influence the number concentration of SSA particles (section 3.3), the CCN activity of these particles was independent of the original OM. Several
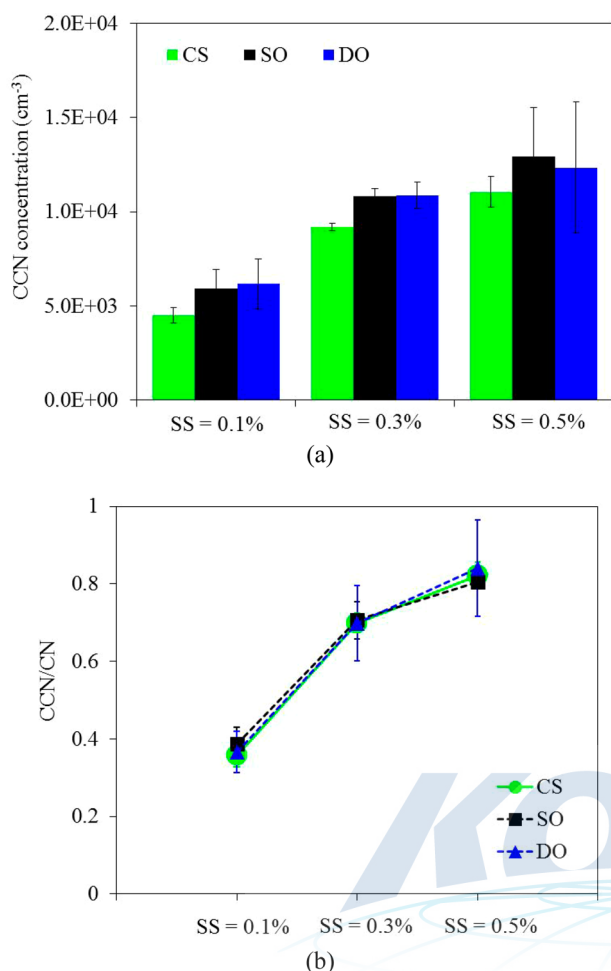
Figure 4. Comparison of (a) CCN concentrations and (b) CCN activity of SSA generated from CS, SO, and DO samples under different supersaturation conditions. CCN activity is defined as the ratio of the number concentration of particles that activated to become CCN at a given supersaturation to total particle number (CN).

sea spray tank studies have also shown that the effect of organic enrichment on CCN activity is not significant.[30−32,67] Modini et al.[68] reported that changes in seawater OM content, despite having an impact on SSA production, do not affect CCN concentrations at a similar space. In addition, Moore et al.[32] found that mixture of NaCl and pure OM (e.g., oleic acid) increased in CCN activity due to a decrease in surface tension. In contrast, an artificial seawater solution with diverse microorganisms (both *Synechococcus* and *Ostreococcus*) produced particles containing ∼34 times more carbon than particles produced from pure artificial seawater; yet, the microorganisms did not affect the CCN activity because the decrease in surface tension could be offset by the decrease in soluble salt.[32] Thus, we hypothesized that SSA particles generated from CS, SO, and DO contain a variety of different organic species and biological particles that produced offsetting effects, resulting in minor change in the CCN activity. However, further studies are needed to identify the influence of chemical composition and mixing state of individual SSA particles on CCN properties.

4.1. ATMOSPHERIC IMPLICATIONS

By performing aerosol generation chamber experiments in the Arctic Ocean, we explored the relationship between various types of OM in surface seawater and the physical properties of SSA, including their activation as CCN, under different environmental conditions (coastal sample with riverine inputs vs ocean sample without riverine inputs). This study reveals that both sea salt and OM contents of seawater have an influence on primary aerosol emission. In coastal Arctic surface waters, riverine OM enhances the number concentration of SSA particles. In offshore oceanic waters, autochthonous particulate OM, including microbial cells, add to sea salt as SSA sources.

There are a few limitations of the present study that warrant further exploration. First, the river-derived organic matter that contributes to the production of SSA in the coastal region includes both terrestrial DOM and primary production. The use of specific tracers should allow assessing the relative importance of each. Second, we still do not fully know the factors controlling SSA numbers from offshore ocean waters. The abundance and diversity of OM in the ocean samples differ from those in the coastal samples. Thus, further laboratory chamber studies are required in the future, using two different types of organic solutions across mixing proportions and concentration gradients. For instance, one would comprise a riverine organic solution (humic and fulvic substances), and another would be an oceanic organic solution (e.g., organic substances released by natural phytoplankton populations, polysaccharides, proteins, and bacteria). Controlled proportions and gradients should be compared to SSA numbers and CCN activity to further assess the direct impact of riverine inputs on aerosols and clouds.

The Arctic Ocean has the most extensive shelves of any ocean, covering about 50% of its total area.[69] Relative to other oceans, river inflow is of special importance in the Arctic Ocean, which contains only 1.0% of global ocean volume but receives 11% of global river discharge.[70] The largest part of the Arctic freshwater originates from six major pan-Arctic rivers: Ob' at Salekhard, Yenisey at Dudinka, Lena at Zhigansk, Kolyma at Cherskiy, Yukon at Pilot Station, and Mackenzie at Tsiigehtchic or Inuvik.[47] In addition, river-monitoring data indicate that the average annual discharge of freshwater from the six rivers to the Arctic Ocean increased by 7% from 1936 to 1999.[71] These six major rivers cover ∼61% of the 20.5×10^6 km^2 total pan-arctic watersheds.[47] The large river inputs to the Arctic Ocean strongly influence the coastal salinity structure and carbon cycle. Increasing river discharge leads to a decrease in the sea surface salinity and an increase in the load of terrestrial DOM and nutrients in surface waters.[72] Benner et al.[73] reported that surface waters of the Arctic Ocean have the highest concentrations of DOC and terrestrial DOM of all ocean basins. They found that the large contribution of terrestrial DOM from Arctic rivers is responsible for the elevated concentrations of DOC in Arctic surface waters. The total amount of DOC discharged by rivers into the Arctic Ocean is $18-26 \times 10^{12}$ g C yr^{-1} and similar to that of the Amazon.[74] The Artic riverine organic matter can be directly emitted from surface seawater into the atmosphere via bubble bursting. In global models, global organic emissions associated with SSA have been estimated from the correlation between satellite-derived Chl *a* and the organic carbon content of SSA.[3,75] Our work suggests that, without considering the

riverine organic matter, Chl a-based emissions underpredict the organic content of SSA in regions where riverine inputs are significant. Our findings suggest that river-driven organic matter, especially terrestrial DOM and TEP, must be incorporated into future global coupled ocean-atmospheric models to improve the accuracy in predicting the organic enrichment of SSA.

■ ASSOCIATED CONTENT

Ⓢ Supporting Information

The Supporting Information is available free of charge on the ACS Publications website at DOI: 10.1021/acs.est.9b03399.

> Figures and tables showing seawater properties and location of 9 different sampling site: detailed measurements of SSA properties, average size distribution of SSA particles, concentration of OM tracers in surface seawater, correlations of DOC to CDOM and seawater salinity, typical EEM spectra of DOM samples, correlation between TEP and N (3 nm−1 μm)/salinity, and relationships between CCN concentrations of SSA and concentrations of various organic matter in seawater (PDF)

■ AUTHOR INFORMATION

Corresponding Author
*E-mail: jypark@kopri.re.kr.

ORCID Ⓞ
Jiyeon Park: 0000-0002-1761-9657
Manuel Dall'Osto: 0000-0003-4203-894X
Young Jun Yoon: 0000-0002-3792-4624

Author Contributions
▽Jiyeon Park and Manuel Dall'Osto contributed equally to this work.

Notes
The authors declare no competing financial interest.

■ ACKNOWLEDGMENTS

■ REFERENCES

(1) ACIA. Arctic Climate Impact Assessment, chap. 2, p 23, Cambridge University Press: New York, USA, 2005.

(2) Cavalieri, D. J.; Parkinson, C. L. Arctic sea ice variability and trends, 1979−2010. *Cryosphere* **2012**, *6*, 881−889.

(3) Gantt, B.; Meskhidze, N.; Kamykowski, D. A new physically-based quantification of marine isoprene and primary organic aerosol emissions. *Atmos. Chem. Phys.* **2009**, *9* (14), 4915−4927.

(4) O'Dowd, C. D.; de Leeuw, G. Marine aerosol production: a review of the current knowledge. *Philos. Trans. R. Soc., A* **2007**, *365* (1856), 1753−1774.

(5) Prather, K. A.; Bertram, T. H.; Grassian, V. H.; Deane, G. B.; Stokes, M. D.; DeMott, P. J.; Aluwihare, L. I.; Palenik, B. P.; Azam, F.; Seinfeld, J. H.; Moffet, R. C.; Molina, M. J.; Cappa, C. D.; Geiger, F. M.; Roberts, G. C.; Russell, L. M.; Ault, A. P.; Baltrusaitis, J.; Collins, D. B.; Corrigan, C. E.; Cuadra-Rodriguez, L. A.; Ebben, C. J.; Forestieri, S. D.; Guasco, T. L.; Hersey, S. P.; Kim, M. J.; Lambert, W. F.; Modini, R. L.; Mui, W.; Pedler, B. E.; Ruppel, M. J.; Ryder, O. S.; Schoepp, N. G.; Sullivan, R. C.; Zhao, D. Bringing the ocean into the laboratory to probe the chemical complexity of sea spray aerosol. *Proc. Natl. Acad. Sci. U. S. A.* **2013**, *110* (19), 7550−7555.

(6) Partanen, A. I.; Dunne, E. M.; Bergman, T.; Laakso, A.; Kokkola, H.; Ovadnevaite, J.; Sogacheva, L.; Baisnée, D.; Sciare, J.; Manders, A.; O'Dowd, C.; de Leeuw, G.; Korhonen, H. Global modelling of direct and indirect effects of sea spray aerosol using a source function encapsulating wave state. *Atmos. Chem. Phys.* **2014**, *14* (21), 11731−11752.

(7) Vaida, V. Ocean Sea Spray, Clouds, and Climate. *ACS Cent. Sci.* **2015**, *1* (3), 112−114.

(8) Wilson, T. W.; Ladino, L. A.; Alpert, P. A.; Breckels, M. N.; Brooks, I. M.; Browse, J.; Burrows, S. M.; Carslaw, K. S.; Huffman, J. A.; Judd, C.; Kilthau, W. P.; Mason, R. H.; McFiggans, G.; Miller, L. A.; Nájera, J. J.; Polishchuk, E.; Rae, S.; Schiller, C. L.; Si, M.; Temprado, J. V.; Whale, T. F.; Wong, J. P. S.; Wurl, O.; Yakobi-Hancock, J. D.; Abbatt, J. P. D.; Aller, J. Y.; Bertram, A. K.; Knopf, D. A.; Murray, B. J. A marine biogenic source of atmospheric ice-nucleating particles. *Nature* **2015**, *525*, 234.

(9) Cunliffe, M.; Engel, A.; Frka, S.; Gašparović, B.; Guitart, C.; Murrell, J. C.; Salter, M.; Stolle, C.; Upstill-Goddard, R.; Wurl, O. Sea surface microlayers: A unified physicochemical and biological perspective of the air−ocean interface. *Prog. Oceanogr.* **2013**, *109*, 104−116.

(10) Leck, C.; Bigg, E. K. Biogenic particles in the surface microlayer and overlaying atmosphere in the central Arctic Ocean during summer. *Tellus B* **2005**, *57* (4), 305−316.

(11) O'Dowd, C. D.; Facchini, M. C.; Cavalli, F.; Ceburnis, D.; Mircea, M.; Decesari, S.; Fuzzi, S.; Yoon, Y. J.; Putaud, J.-P. Biogenically driven organic contribution to marine aerosol. *Nature* **2004**, *431*, 676.

(12) Facchini, M. C.; Rinaldi, M.; Decesari, S.; Carbone, C.; Finessi, E.; Mircea, M.; Fuzzi, S.; Ceburnis, D.; Flanagan, R.; Nilsson, E. D.; de Leeuw, G.; Martino, M.; Woeltjen, J.; O'Dowd, C. D. Primary submicron marine aerosol dominated by insoluble organic colloids and aggregates. *Geophys. Res. Lett.* **2008**, *35* (17), L17814.

(13) Ceburnis, D.; O'Dowd, C. D.; Jennings, G. S.; Facchini, M. C.; Emblico, L.; Decesari, S.; Fuzzi, S.; Sakalys, J. Marine aerosol chemistry gradients: Elucidating primary and secondary processes and fluxes. *Geophys. Res.* **2008**, *35* (7), L07804.

(14) Alpert, P. A.; Kilthau, W. P.; Bothe, D. W.; Radway, J. C.; Aller, J. Y.; Knopf, D. A. The influence of marine microbial activities on aerosol production: A laboratory mesocosm study. *J. Geophys. Res.-Atmos* **2015**, *120*, 8841−8860.

(15) Aller, J. Y.; Radway, J. C.; Kilthau, W. P.; Bothe, D. W.; Wilson, T. W.; Vaillancourt, R. D.; Quinn, P. K.; Coffman, D. J.; Murray, B. J.; Knopf, D. A. Size-resolved characterization of the polysaccharidic and proteinaceous components of sea spray aerosol. *Atmos. Environ.* **2017**, *154*, 331−347.

(16) Shaw, P. M.; Russell, L. M.; Jefferson, A.; Quinn, P. K. Arctic organic aerosol measurements show particles from mixed combustion in spring haze and from frost flowers in winter. *Geophys. Res.* **2010**, *37* (10), L10803.

(17) Russell, L. M.; Hawkins, L. N.; Frossard, A. A.; Quinn, P. K.; Bates, T. S. Carbohydrate-like composition of submicron atmospheric particles and their production from ocean bubble bursting. *Proc. Natl. Acad. Sci. U. S. A.* **2010**, *107* (15), 6652−6657.

(18) Fu, P. Q.; Kawamura, K.; Chen, J.; Charrière, B.; Sempéré, R. Organic molecular composition of marine aerosols over the Arctic Ocean in summer: contributions of primary emission and secondary aerosol formation. *Biogeosciences* **2013**, *10*, 653−667.

(19) Chang, R. Y.-W.; Leck, C.; Graus, M.; Müller, M.; Paatero, J.; Burkhart, J. F.; Stohl, A.; Orr, L. H.; Hayden, K.; Li, S.-M.; Hansel, A.; Tjernström, M.; Leaitch, W. R.; Abbatt, J. P. D. Aerosol composition and sources in the central Arctic Ocean during ASCOS. *Atmos. Chem. Phys.* **2011**, *11*, 10619−10636.

(20) Hawkins, L. N.; Russell, L. M. Polysaccharides, Proteins, and Phytoplankton Fragments: Four Chemically Distinct Types of Marine Primary Organic Aerosol Classified by Single Particle Spectromicroscopy. *Adv. Meteorol.* **2010**, *2010* (14), 612132.

(21) Hood, E.; Battin, T. J.; Fellman, J.; O'Neel, S.; Spencer, R. G. M. Storage and release of organic carbon from glaciers and ice sheets. *Nat. Geosci.* **2015**, *8*, 91.

(22) Rudels, B. Arctic Ocean circulation, processes and water masses: A description of observations and ideas with focus on the period prior to the International Polar Year 2007−2009. *Prog. Oceanogr.* **2015**, *132*, 22−67.

(23) Le Fouest, V.; Matsuoka, A.; Manizza, M.; Shernetsky, M.; Tremblay, B.; Babin, M. Towards an assessment of riverine dissolved organic carbon in surface waters of the western Arctic Ocean based on remote sensing and biogeochemical modeling. *Biogeosciences* **2018**, *15*, 1335−1346.

(24) Quinn, P. K.; Collins, D. B.; Grassian, V. H.; Prather, K. A.; Bates, T. S. Chemistry and Related Properties of Freshly Emitted Sea Spray Aerosol. *Chem. Rev.* **2015**, *115* (10), 4383−4399.

(25) Nebbioso, A.; Piccolo, A. Molecular characterization of dissolved organic matter (DOM): a critical review. *Anal. Bioanal. Chem.* **2013**, *405* (1), 109−124.

(26) Vignati, E.; Facchini, M. C.; Rinaldi, M.; Scannell, C.; Ceburnis, D.; Sciare, J.; Kanakidou, M.; Myriokefalitakis, S.; Dentener, F.; O'Dowd, C. D. Global scale emission and distribution of sea-spray aerosol: Sea-salt and organic enrichment. *Atmos. Environ.* **2010**, *44* (5), 670−677.

(27) Quinn, P. K.; Bates, T. S.; Schulz, K. S.; Coffman, D. J.; Frossard, A. A.; Russell, L. M.; Keene, W. C.; Kieber, D. J. Contribution of sea surface carbon pool to organic matter enrichment in sea spray aerosol. *Nat. Geosci.* **2014**, *7*, 228.

(28) Hultin, K. A. H.; Krejci, R.; Pinhassi, J.; Gomez-Consarnau, L.; Mårtensson, E. M.; Hagström, Å.; Nilsson, E. D. Aerosol and bacterial emissions from Baltic Seawater. *Atmos. Res.* **2011**, *99* (1), 1−14.

(29) Fahlgren, C.; Gómez-Consarnau, L.; Zábori, J.; Lindh, M. V.; Krejci, R.; Mårtensson, E. M.; Nilsson, D.; Pinhassi, J. Seawater mesocosm experiments in the Arctic uncover differential transfer of marine bacteria to aerosols. *Environ. Microbiol. Rep.* **2015**, *7* (3), 460−470.

(30) O'Dowd, C.; Ceburnis, D.; Ovadnevaite, J.; Bialek, J.; Stengel, D. B.; Zacharias, M.; Nitschke, U.; Connan, S.; Rinaldi, M.; Fuzzi, S.; Decesari, S.; Cristina Facchini, M.; Marullo, S.; Santoleri, R.; Dell'Anno, A.; Corinaldesi, C.; Tangherlini, M.; Danovaro, R. Connecting marine productivity to sea-spray via nanoscale biological processes: Phytoplankton Dance or Death Disco? *Sci. Rep.* **2015**, *5*, 14883.

(31) Ovadnevaite, J.; Ceburnis, D.; Martucci, G.; Bialek, J.; Monahan, C.; Rinaldi, M.; Facchini, M. C.; Berresheim, H.; Worsnop, D. R.; O'Dowd, C. Primary marine organic aerosol: A dichotomy of low hygroscopicity and high CCN activity. *Geophys. Res. Lett.* **2011**, *38* (21), L21806.

(32) Moore, M. J. K.; Furutani, H.; Roberts, G. C.; Moffet, R. C.; Gilles, M. K.; Palenik, B.; Prather, K. A. Effect of organic compounds on cloud condensation nuclei (CCN) activity of sea spray aerosol produced by bubble bursting. *Atmos. Environ.* **2011**, *45* (39), 7462−7469.

(33) Fuentes, E.; Coe, H.; Green, D.; McFiggans, G. On the impacts of phytoplankton-derived organic matter on the properties of the primary marine aerosol − Part 2: Composition, hygroscopicity and cloud condensation activity. *Atmos. Chem. Phys.* **2011**, *11* (6), 2585−2602.

(34) King, S. M.; Butcher, A. C.; Rosenoern, T.; Coz, E.; Lieke, K. I.; de Leeuw, G.; Nilsson, E. D.; Bilde, M. Investigating Primary Marine Aerosol Properties: CCN Activity of Sea Salt and Mixed Inorganic−Organic Particles. *Environ. Sci. Technol.* **2012**, *46* (19), 10405−10412.

(35) Gantt, B.; Xu, J.; Meskhidze, N.; Zhang, Y.; Nenes, A.; Ghan, S. J.; Liu, X.; Easter, R.; Zaveri, R. Global distribution and climate forcing of marine organic aerosol − Part 2: Effects on cloud properties and radiative forcing. *Atmos. Chem. Phys.* **2012**, *12*, 6555−6563.

(36) Ovadnevaite, J.; Zuend, A.; Laaksonen, A.; Sanchez, K. J.; Roberts, G.; Ceburnis, D.; Decesari, S.; Rinaldi, M.; Hodas, N.; Facchini, M. C.; Seinfeld, J. H.; O' Dowd, C. Surface tension prevails over solute effect in organic-influenced cloud droplet activation. *Nature* **2017**, *546*, 637−641.

(37) Sellegri, K.; O'Dowd, C. D.; Yoon, Y. J.; Jennings, S. G.; de Leeuw, G. Surfactants and submicron sea spray generation. *J. Geophys. Res.-Atmos.* **2006**, *111* (D22), D22215.

(38) Fuentes, E.; Coe, H.; Green, D.; de Leeuw, G.; McFiggans, G. Laboratory-generated primary marine aerosol via bubble-bursting and atomization. *Atmos. Meas. Tech.* **2010**, *3* (1), 141−162.

(39) Tritscher, T.; Koched, A.; Han, H.-S.; Filimundi, E.; Johnson, T.; Elzey, S.; Avenido, A.; Kykal, C.; Bischof, O. F. Multi-Instrument Manager Tool for Data Acquisition and Merging of Optical and Electrical Mobility Size Distributions. *J. Phys.: Conf. Ser.* **2015**, *617*, 012013.

(40) Zapata, M; Rodriguez, F; Garrido, J. Separation of chlorophylls and carotenoids from marine phytoplankton: a new HPLC method using a reversed phase C8 column and pyridine-containing mobile phases. *Mar. Ecol.: Prog. Ser.* **2000**, *195*, 29−45.

(41) Jeffrey, S. W.; Mantoura, R. F. C.; Wright, S. W. In *Phytoplankton Pigments in Oceanography: Guidelines to Modern Methods*; Jeffrey, S. W., Mantoura, R. F. C., Wright, S. W., Eds.; UNESCO Publishing: Paris, 1997.

(42) Kowalczuk, P.; Stoń-Egiert, J.; Cooper, W. J.; Whitehead, R. F.; Durako, M. J. Characterization of chromophoric dissolved organic matter (CDOM) in the Baltic Sea by excitation emission matrix fluorescence spectroscopy. *Mar. Chem.* **2005**, *96* (3), 273−292.

(43) Coble, P. G. Characterization of marine and terrestrial DOM in seawater using excitation-emission matrix spectroscopy. *Mar. Chem.* **1996**, *51* (4), 325−346.

(44) Passow, U.; Alldredge, A. L. A dye-binding assay for the spectrophotometric measurement of transparent exopolymer particles (TEP). *Limnol. Oceanogr.* **1995**, *40* (7), 1326−1335.

(45) Cisternas-Novoa, C.; Lee, C.; Engel, A. Transparent exopolymer particles (TEP) and Coomassie stainable particles (CSP): Differences between their origin and vertical distributions in the ocean. *Mar. Chem.* **2015**, *175*, 56−71.

(46) Noble, R.; Fuhrman, J. Use of SYBR Green I for rapid epifluorescence counts of marine viruses and bacteria. *Aquat. Microb. Ecol.* **1998**, *14*, 113−118.

(47) Holmes, R. M.; McClelland, J. W.; Peterson, B. J.; Tank, S. E.; Bulygina, E.; Eglinton, T. I.; Gordeev, V. V.; Gurtovaya, T. Y.; Raymond, P. A.; Repeta, D. J.; Staples, R.; Striegl, R. G.; Zhulidov, A. V.; Zimov, S. A. Seasonal and Annual Fluxes of Nutrients and Organic Matter from Large Rivers to the Arctic Ocean and Surrounding Seas. *Estuaries Coasts* **2012**, *35* (2), 369−382.

(48) Stroh, J. N.; Panteleev, G.; Kirillov, S.; Makhotin, M.; Shakhova, N. Sea surface temperature and salinity product comparison against external in situ data in the Arctic Ocean. *J. Geophys. Res.-Oceans* **2015**, *120* (11), 7223−7236.

(49) Martensson, E. M.; Nilsson, E. D.; de Leeuw, G.; Cohen, L. H.; Hansson, H.-C. Laboratory simulations and parameterization of the primary marine aerosol production. *J. Geophys. Res.- Atmos* **2003**, *108* (D9), 4297.

(50) Park, J. Y.; Lim, S.; Park, K. Mixing State of Submicrometer Sea Spray Particles Enriched by Insoluble Species in Bubble-Bursting Experiments. *J. Atmos. Oceanic Technol.* **2014**, *31* (1), 93−104.

(51) Zábori, J.; Krejci, R.; Ekman, A. M. L.; Mårtensson, E. M.; Ström, J.; de Leeuw, G.; Nilsson, E. D. Wintertime Arctic Ocean sea water properties and primary marine aerosol concentrations. *Atmos. Chem. Phys.* **2012**, *12*, 10405−10421.

(52) Tanaka, K.; Takesue, N.; Nishioka, J.; Kondo, Y.; Ooki, A.; Kuma, K.; Hirawake, T.; Yamashita, Y. The conservative behavior of dissolved organic carbon in surface waters of the southern Chukchi Sea, Arctic Ocean, during early summer. *Sci. Rep.* **2016**, *6*, 34123.

(53) Shen, Y.; Fichot, C.; Benner, R. Dissolved organic matter composition and bioavailability reflect ecosystem productivity in the Western Arctic Ocean. *Biogeosciences* **2012**, *9*, 4993−5005.

(54) Kaiser, K.; Canedo-Oropeza, M.; McMahon, R.; Amon, R. M. W. Origins and transformations of dissolved organic matter in large Arctic rivers. *Sci. Rep.* **2017**, *7*, 13064.

(55) Mann, P. J.; Spencer, R. G. M.; Hernes, P. J.; Six, J.; Aiken, G. R.; Tank, S. E.; McClelland, J. W.; Butler, K. D.; Dyda, R. Y.; Holmes, R. M. Pan-Arctic Trends in Terrestrial Dissolved Organic Matter from Optical Measurements. *Fornt. Earth Sci.* **2016**, *4* (25), 1−18.

(56) Tzortziou, M.; Zeri, C.; Dimitriou, E.; Ding, Y.; Jaffé, R.; Anagnostou, E.; Pitta, E.; Mentzafou, A. Colored dissolved organic matter dynamics and anthropogenic influences in a major transboundary river and its coastal wetland. *Limnol. Oceanogr.* **2015**, *60* (4), 1222−1240.

(57) Slonecker, E. T.; Jones, D. K.; Pellerin, B. A. The new Landsat 8 potential for remote sensing of colored dissolved organic matter (CDOM). *Mar. Pollut. Bull.* **2016**, *107* (2), 518−527.

(58) Panagiotopoulos, C.; Sempéré, R.; Jacq, V.; Charrière, B. Composition and distribution of dissolved carbohydrates in the Beaufort Sea Mackenzie margin (Arctic Ocean). *Mar. Chem.* **2014**, *166*, 92−102.

(59) Raymond, P. A.; McClelland, J. W.; Holmes, R. M.; Zhulidov, A. V.; Mull, K.; Peterson, B. J.; Striegl, R. G.; Aiken, G. R.; Gurtovaya, T. Y. Flux and age of dissolved organic carbon exported to the Arctic Ocean: A carbon isotopic study of the five largest arctic rivers. *GLOBAL BIOGEOCHEM CY* **2007**, *21*, GB4011.

(60) CLASEN, J. L.; BRIGDEN, S. M.; PAYET, J. P.; SUTTLE, C. A. Evidence that viral abundance across oceans and lakes is driven by different biological factors. *Freshwater Biol.* **2008**, *53* (6), 1090−1100.

(61) Verdugo, P.; Alldredge, A. L.; Azam, F.; Kirchman, D. L.; Passow, U.; Santschi, P. H. The oceanic gel phase: a bridge in the DOM−POM continuum. *Mar. Chem.* **2004**, *92* (1), 67−85.

(62) Chin, W.-C.; Orellana, M. V.; Verdugo, P. Spontaneous assembly of marine dissolved organic matter into polymer gels. *Nature* **1998**, *391*, 568.

(63) Orellana, M. V.; Matrai, P. A.; Leck, C.; Rauschenberg, C. D.; Lee, A. M.; Coz, E. Marine microgels as a source of cloud condensation nuclei in the high Arctic. *Proc. Natl. Acad. Sci. U. S. A.* **2011**, *108* (33), 13612−13617.

(64) Coble, P. G. Marine Optical Biogeochemistry: The Chemistry of Ocean Color. *Chem. Rev.* **2007**, *107* (2), 402−418.

(65) Miyazaki, Y.; Yamashita, Y.; Kawana, K.; Tachibana, E.; Kagami, S.; Mochida, M.; Suzuki, K.; Nishioka, J. Chemical transfer of dissolved organic matter from surface seawater to sea spray water-soluble organic aerosol in the marine atmosphere. *Sci. Rep.* **2018**, *8* (1), 14861.

(66) Rinaldi, M.; Decesari, S.; Finessi, E.; Giulianelli, L.; Carbone, C.; Fuzzi, S.; O'Dowd, C. D.; Ceburnis, D.; Facchini, M. C. Primary and secondary organic marine aerosol and oceanic bioloigcal activity: Rescent results and new perspectivies for future studies. *Adv. Meteorol.* **2010**, *2010*, 310682.

(67) Moore, R. H.; Ingall, E. D.; Sorooshian, A.; Nenes, A. Molar mass, surface tension, and droplet growth kinetics of marine organics from measurements of CCN activity. *Geophys. Res. Lett.* **2008**, *35* (7), L07801.

(68) Modini, R. L.; Harris, B.; Ristovski, Z. D. The organic fraction of bubble-generated, accumulation mode Sea Spray Aerosol (SSA). *Atmos. Chem. Phys.* **2010**, *10* (6), 2867−2877.

(69) Boeuf, D.; Humily, F.; Jeanthon, C. Diversity of Arctic pelagic Bacteria with an emphasis on photoheterotrophs: a review. *Biogeosciences* **2014**, *11* (12), 3309−3322.

(70) Shiklomanov, I. A.; Shiklomanov, A. I.; Lammers, R. B.; Peterson, B. J.; Vorosmarty, C. J. The Dynamics of River Water Inflow to the Arctic Ocean. *Freshwater Budget of the Arctic Ocea* **2000**, 281−296.

(71) Peterson, B. J.; Holmes, R. M.; McClelland, J. W.; Vörösmarty, C. J.; Lammers, R. B.; Shiklomanov, A. I.; Shiklomanov, I. A.; Rahmstorf, S. Increasing River Discharge to the Arctic. *Science* **2002**, *298* (5601), 2171−2173.

(72) McClelland, J. W.; Déry, S. J.; Peterson, B. J.; Holmes, R. M.; Wood, E. F. A pan-arctic evaluation of changes in river discharge during the latter half of the 20th century. *Geophys. Res. Lett.* **2006**, *33* (6), L06715.

(73) Benner, R.; Louchouarn, P.; Amon, R. M. W. Terrigenous dissolved organic matter in the Arctic Ocean and its transport to surface and deep waters of the North Atlantic. *Global Biogeochem. Cy.* **2005**, *19* (2), GB2025.

(74) Dittmar, T.; Kattner, G. The biogeochemistry of the river and shelf ecosystem of the Arctic Ocean: a review. *Mar. Chem.* **2003**, *83* (3), 103−120.

(75) O'Dowd, C. D.; Langmann, B.; Varghese, S.; Scannell, C.; Ceburnis, D.; Facchini, M. C. A combined organic-inorganic sea-spray source function. *Geophys. Res. Lett.* **2008**, *35* (1), L01801.